RESEARCH ARTICLE

Open Access

Open Data

Open Code

Modelling the impact of the macroalgae *Asparagopsis taxiformis* on rumen microbial fermentation and methane production

Rafael Muñoz-Tamayo[1]* , Juana C. Chagas[2], Mohammad Ramin[2], and Sophie J. Krizsan[2]

*Correspondence:
Rafael.munoz-tamayo@inrae.fr

[1] Université Paris-Saclay, INRAE, AgroParisTech, UMR Modélisation Systémique Appliquée aux Ruminants, 75005, Paris, France.
[2] Department of Agricultural Research for Northern Sweden, Swedish University of Agricultural Sciences (SLU), Skogsmarksgränd, 90183 Umeå, Sweden.

Abstract

Background: The red macroalgae *Asparagopsis taxiformis* is a potent natural supplement for reducing methane production from cattle. *A. taxiformis* contains several anti-methanogenic compounds including bromoform that inhibits directly methanogenesis. The positive and adverse effects of *A. taxiformis* on the rumen microbiota are dose-dependent and operate in a dynamic fashion. It is therefore key to characterize the dynamic response of the rumen microbial fermentation for identifying optimal conditions on the use of *A. taxiformis* as a dietary supplement for methane mitigation. Accordingly, the objective of this work was to model the effect of *A. taxiformis* supplementation on the rumen microbial fermentation under *in vitro* conditions. We adapted a published mathematical model of rumen microbial fermentation to account for *A. taxiformis* supplementation. We modelled the impact of *A. taxiformis* on the fermentation and methane production by two mechanisms, namely (i) direct inhibition of the growth rate of methanogens by bromoform and (ii) hydrogen control on sugars utilization and on the flux allocation towards volatile fatty acids production. We calibrated our model using a multi-experiment estimation approach that integrated experimental data with six macroalgae supplementation levels from a published *in vitro* study assessing the dose-response impact of *A. taxiformis* on rumen fermentation.

Results: our model captured satisfactorily the effect of *A. taxiformis* on the dynamic profile of rumen microbial fermentation for the six supplementation levels of *A. taxiformis* with an average determination coefficient of 0.88 and an average coefficient of variation of the root mean squared error of 15.2% for acetate, butyrate, propionate, ammonia and methane.

Conclusions: our results indicated the potential of our model as prediction tool for assessing the impact of additives such as seaweeds on the rumen microbial fermentation and methane production *in vitro*. Additional dynamic data on hydrogen and bromoform are required to validate our model structure and look for model structure improvements. We expect this model development can be useful to help the design of sustainable nutritional strategies promoting healthy rumen function and low environmental footprint.

Keywords: greenhouse gas mitigation, hydrogen control, methane inhibitors, methane mitigation, red seaweed, rumen fermentation, rumen microbiota, rumen model.

1. Background

Some macroalgae (seaweeds) have the potential to be used as natural supplement for reducing methane (CH_4) production from cattle (Wang *et al.*, 2008; Dubois *et al.*, 2013; Maia *et al.*, 2016). This anti-methanogenic activity adds value to the nutritional and healthy promoting properties of macroalgae in livestock diets (Evans and Critchley, 2014; Makkar *et al.*, 2016). The species of the red macroalgae *Asparagopsis* have proven a strong anti-methanogenic effect both *in vitro* (Machado *et al.*, 2014) and *in vivo* (Roque *et al.*, 2019). In particular, *Asparagopsis taxiformis* appears as the most potent species for methane mitigation with studies reporting a reduction in enteric methane up to 80% in sheep (Li *et al.*, 2016) and up to 80% and 98% in beef cattle (Kinley *et al.*, 2020; Roque *et al.*, 2020). The anti-methanogenic power of *A. taxiformis* results from the action of its multiple secondary metabolites with antimicrobial activities, being bromoform the most abundant anti-methanogenic compound (Machado *et al.*, 2016b). It should be said, however, that despite the promising anti-methanogenic capacity of bromoform, the feasibility of supplying bromoform-containing macroalgae requires a global assessment to insure safety of feeding and low environmental footprint from the algae processing, since bromoform can be toxic to the environment and can impair human health (Beauchemin *et al.*, 2020).

Bromoform is released from specialised gland cells of the macroalage (Paul *et al.*, 2006) in to the culture medium. The mode of action of the anti-methanogenic activity of bromoform is similar to that described for bromochloromethane (Denman *et al.*, 2007), following the mechanism suggested for halogenated hydrocarbons (Wood *et al.*, 1968; Czerkawski and Breckenridge, 1975). Accordingly, bromoform inhibits the cobamid dependent methyl-transfer reactions that lead to methane formation. In addition to the direct effect on the methanogenesis, the antimicrobial activity of *A. taxiformis* impacts the fermentation profile (*e.g.,* acetate:propionate ratio) and the structure of the rumen microbiota (*e.g.,* the relative abundance of methanogens) (Machado *et al.*, 2018; Roque *et al.*, 2019). Fermentation changes may have detrimental effects on animal health and productivity (Chalupa, 1977; Li *et al.*, 2016). Detrimental effects might include deterioration of the ruminal mucosa and the transfer of bromoform to tissues, blood and milk. Previous studies have not detected bromoform in animal tissues (Li *et al.*, 2016; Kinley *et al.*, 2020; Roque *et al.*, 2020). The positive and adverse effects of *A. taxiformis* on the rumen microbiota are dose-dependent (Machado *et al.*, 2016a) and operate in a dynamic fashion. It is therefore key to characterize the dynamic response of the rumen microbial fermentation for identifying optimal conditions on the use of the *A. taxiformis* as a dietary supplement for methane mitigation. The development of dynamic mathematical models provides valuable tools for the assessment of feeding and mitigation strategies (Ellis *et al.*, 2012) including developments in the manipulation of the flows of hydrogen to control rumen fermentation (Ungerfeld, 2020). Progress on rumen modelling including a better representation of the rumen microbiota and the representation of additives on the fermentation is central for the deployment of predictive tools that can guide microbial manipulation strategies for sustainable livestock production (Huws *et al.*, 2018). Accordingly, the objective of this work was to model the effect of *A. taxiformis* supplementation on the dynamics of rumen microbial fermentation under *in vitro* conditions. We adapted a published rumen fermentation model (Muñoz-Tamayo *et al.*, 2016) to account for the impact of *A. taxiformis* on rumen fermentation and methane production evaluated *in vitro* at six supplementation levels (Chagas *et al.*, 2019).

2. Methods

2.1.   Experimental data

Model calibration was performed using experimental data from an *in vitro* batch study assessing the dose-response impact of *A. taxiformis* on fermentation and methane production (Chagas *et al.*, 2019). In such a study, *A. taxiformis* with 6.84 mg/g DM bromoform concentration was supplemented at six treatment levels (0, 0.06, 0.13, 0.25, 0.5, and 1.0 % of diet organic matter; OM). All experimental treatments were composed of a control diet consisted of timothy grass (*Phleum pratense*), rolled barley (*Hordeum vulgare*), and rapeseed (*Brassica napus*) meal in a ratio of 545:363:92 g/kg diet dry matter (DM) presenting chemical composition as 944 g/kg OM, 160 g/kg crude protein (CP) and 387 g/kg neutral detergent fiber (NDF). Prior to each *in vitro* incubation, dried individual ingredients milled at 1 mm were weighted into serum bottles totalizing 1000 mg substrate on DM basis. The incubation was carried out with rumen inoculum from two lactating Swedish Red cows cannulated in the rumen, fed ad libitum on a diet of 600 g/kg grass silage and 400 g/kg concentrate on DM basis. Diet samples were incubated for 48 h in 60 ml of buffered rumen fluid (rumen fluid:buffer ratio of 1:4 by volume) as described by Chagas et al. (2019). The *in vitro* batch fermentation was run in a fully automated system that allows continuous recording of gas production (Ramin and Huhtanen, 2012).

Methane production, acetate, butyrate, propionate, and ammonia were measured throughout the incubation period. Methane was measured at 0, 2, 4, 8, 24, 36 and 48 h according to (Ramin and Huhtanen, 2012). Gas production was measured using a fully automated system (Gas Production Recorder, GPR-2, Version 1.0 2015, Wageningen UR), with readings made every 12 min and corrected to the normal air pressure (101.3 kPa). Methane concentration was determined with a Varian Star 3400 CX gas chromatograph (Varian Analytical Instruments, Walnut Creek, CA, USA) equipped with a thermal conductivity detector. The volatile fatty acids (VFAs) were measured at 0, 8, 24 and 48 h and determined using a Waters Alliance 2795 UPLC system as described by (Puhakka *et al.*, 2016). Ammonia was measured at 0 and 24h and analysed with a continuous flow analyzer (AutoAnalyzer 3 HR, SEAL Analytical Ltd., Southampton, UK) and according to the method provided by SEAL Analytical (Method no. G-102-93 multitest MT7). For model calibration, we only considered data until 24h, since microbial fermentation stopped around this time.

2.2.   Mathematical modelling

We adapted the mathematical model of *in vitro* rumen fermentation developed by (Muñoz-Tamayo *et al.*, 2016) to account for the effect of *A. taxiformis* on the fermentation. This model represents the rumen microbiota by three microbial functional groups (sugar utilisers, amino acid utilisers and methanogens). Hexose monomers are represented by glucose and amino acids are represented by an average amino acid. The model is an aggregated representation of the anaerobic digestion process that comprises the hydrolysis of cell wall carbohydrates (NDF - Neutral Detergent Fiber), non-fiber carbohydrates (NSC – Non Structural Carbohydrates) and proteins, the fermentation of soluble monomers producing the VFAs acetate, butyrate, propionate, and the hydrogenotrophic methanonogenesis. The original model was calibrated using *in vitro* experimental data from (Serment et al., 2016). Figure 1

89 displays a schematic representation of the rumen fermentation model indicating the effect of
90 *A. taxiformis* on the fermentation. We assumed that microbial cells are formed by proteins
91 and non-fiber carbohydrates and that dead microbial cells are recycled as carbon sources in
92 the fermentation.
93
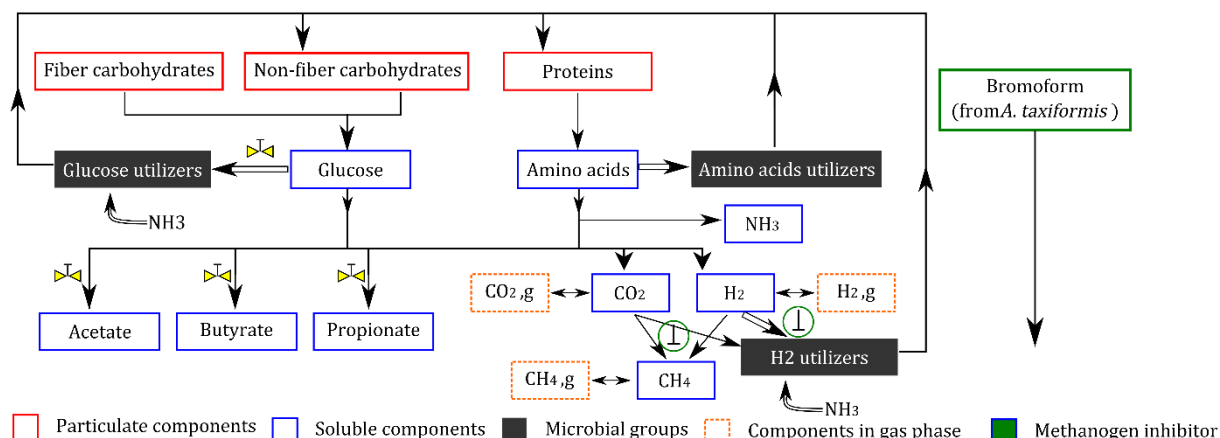
94
Figure 1. Representation of the rumen fermentation model (adapted from (Muñoz-Tamayo *et al.*, 2016)). Hydrolysis of carbohydrates (fiber and non-fiber) and proteins releases respectively sugars and amino acids soluble monomers which are further utilized by the microbiota. The utilization of substrate is directed to product formation (single arrows) and microbial growth (double arrows). Each substrate is utilized by a single microbial functional group. The bromoform contained in *A. taxiformis* produces a direct inhibition of the growth rate of methanogens that results in a reduction of methane production and in an accumulation of hydrogen. The symbol ⊥ indicates the direct effect of the bromoform on the methanogenesis. Hydrogen exerts control on sugars utilization and on the flux allocation towards volatile fatty acids production. The symbol ▷◁ indicates the hydrogen control effect on the rumen fermentation*.

107 The model is derived from mass balance equations of a closed system under the assumption
108 that the protocol of gas sampling does not affect substantially the dynamics of methane and
109 fermentation dynamics. Our model is described in compact way as follows

$$\frac{d\boldsymbol{\xi}}{dt} = \mathbf{S} \cdot \boldsymbol{\rho}(\boldsymbol{\xi}, \mathbf{p}) - \mathbf{g}(\boldsymbol{\xi}, \mathbf{p}) \qquad (1)$$

111 Where $\boldsymbol{\xi}$ is the vector of state variables (metabolites), $\boldsymbol{\rho}(\cdot)$ is a vector function with the kinetic
112 rates of hydrolysis and substrate (sugars, amino acids, hydrogen) utilization. Hydrolysis rates
113 are described by first-order kinetics. Substrate utilization rates are described by the Monod
114 kinetics. $\mathbf{S}$ is the stoichiometry matrix containing the yield factors ($Y_{i,j}$) of each metabolite (i)
115 for each reaction (j), $\mathbf{g}(\cdot)$ is a vector function with the equations representing transport
116 phenomena (liquid–gas transfer), and $\mathbf{p}$ is the vector of the model parameters. The original
117 model has 18 state variables (compartments in Figure. 1) and was implemented in Matlab (the
118 code is accessible at https://doi.org/10.5281/zenodo.4047640). An implementation in R
119 software is also available (Kettle *et al.*, 2018). In the present work, we incorporated an
120 additional state variable to represent the dynamics of bromoform concentration. The original
121 model was extended to account for the impact of *A. taxiformis* on the rumen fermentation.
122 While the original model predicts the pH, we set the pH value to 6.6.
123

124   The impact of *A. taxiformis* on the fermentation and methane production was ascribed to two
125   mechanisms, namely the (i) direct inhibition of the growth rate of methanogens by
126   bromoform and (ii) hydrogen control on sugars utilization and on the flux allocation towards
127   volatile fatty acids production. These aspects are detailed below.
128
129   For the methanogenesis, the reaction rate of hydrogen utilization ρ_{H_2} (mol/(L h)) is given by
130

131
$$\rho_{H_2} = I_{br} \cdot I_{IN} \cdot k_{m,H_2} \frac{s_{H_2}}{K_{s,H_2}+s_{H_2}} x_{H_2} \qquad (2)$$

132
133   where s_{H_2} (mol/L) is the hydrogen concentration in liquid phase, x_{H_2} (mol/L) is the
134   concentration of hydrogen-utilizing microbes (methanogens), k_{m,H_2} (mol/(mol h)) is the
135   maximum specific utilization rate constant of hydrogen and K_{s,H_2} (mol/L) is the Monod affinity
136   constant of hydrogen utilization, and I_{IN} is a nitrogen limitation factor. The kinetic rate is
137   inhibited by the anti-methanogenic compounds of *A. taxiformis*. The factor I_{br} represents this
138   inhibition as function of the bromoform concentration. We used the following sigmoid
139   function to describe I_{br}
140

141
$$I_{br} = 1 - \frac{1}{1+\exp(-p_1 \cdot (s_{br}+p_2))} \qquad (3)$$

142
143   where s_{br} is the bromoform concentration (g/L) and p_1, p_2 are the parameters of the sigmoid
144   function. We included in our model the dynamics of bromoform using a first-order kinetics to
145   take into account that the inhibition of *A. taxiformis* declines on time as a result of the
146   consumption of anti-methanogenic compounds (Kinley *et al.*, 2016). The dynamics of s_{br} is
147

148
$$\frac{ds_{br}}{dt} = -k_{br} \cdot s_{br} \qquad (4)$$

149
150   where k_{br} (1/h) is the kinetic rate constant of bromoform utilization.
151
152   With regard to sugars utilization, we assumed that the effect of *A. taxiformis* is ascribed to
153   hydrogen control due to accumulation of hydrogen resulting from the methanogenesis
154   inhibition. Hydrogen level influences the fermentation pattern (Janssen, 2010). We used the
155   structure proposed by (Mosey, 1983) to account for hydrogen control on sugar utilization and
156   flux allocation. However, we used different parametric functions to those proposed by
157   (Mosey, 1983). The functions proposed by (Mosey, 1983) did not provide satisfactory results.
158
159   In our model, the kinetic rate of sugar utilization is described by
160

161
$$\rho_{su} = I_{H_2} \cdot I_{IN} \cdot k_{m,su} \frac{s_{su}}{K_{s,su}+s_{su}} x_{su} \qquad (5)$$

162   where s_{su} (mol/L) is the concentration of sugars, x_{su} (mol/L), is the concentration of sugar
163   utilisers microbes, $k_{m,su}$ (mol/(mol h) is the maximum specific utilization rate constant of
164   sugars and $K_{s,su}$ (mol/L) is the Monod affinity constant of sugars utilization.
165

5

166   The factor $I_{\mathrm{H_2}}$ describes the hydrogen inhibition:

167

168
$$I_{\mathrm{H_2}} = 1 - \frac{1}{1+\exp\left(-p_3\cdot\left(p_{\mathrm{H_2}}+p_4\right)\right)} \tag{6}$$

169   with $p_{\mathrm{H_2}}$ the hydrogen partial pressure ($p_{\mathrm{H_2}}$).

170

171   In our model, the rumen fermentation is represented by the macroscopic reactions in Table
172   1.

173

174   **Table 1**. Macroscopic reactions used in our model to representing rumen fermentation. For
175   the anabolic reactions of microbial formation, we assume that microbial biomass has the
176   molecular formula $C_5H_7O_2N$.

177

Sugars (glucose) utilization	
$C_6H_{12}O_6 + 2H_2O \rightarrow 2CH_3COOH + 2CO_2 + 4H_2$	R_1
$3C_6H_{12}O_6 \rightarrow 2CH_3COOH + 4CH_3CH_2COOH + 2CO_2 + 2H_2O$	R_2
$C_6H_{12}O_6 \rightarrow CH_3 CH_2CH_2COOH + 2CO_2 + 2H_2$	R_3
$5C_6H_{12}O_6 + 6NH_3 \rightarrow 6C_5H_7O_2N + 18H_2O$	R_4
Amino acid utilization	
$C_5H_{9.8}O_{2.7}N_2 \rightarrow Y_{\mathrm{IN,aa}}NH_3 + (1-Y_{\mathrm{aa}})\cdot\sigma_{\mathrm{ac,aa}} CH_3COOH + (1-Y_{\mathrm{aa}})\cdot\sigma_{\mathrm{pr,aa}} CH_3CH_2COOH + (1-Y_{\mathrm{aa}})\cdot\sigma_{\mathrm{bu,aa}} CH_3 CH_2CH_2COOH + (1-Y_{\mathrm{aa}})\cdot\sigma_{\mathrm{IC,aa}} CO_2 + (1-Y_{\mathrm{aa}})\cdot\sigma_{\mathrm{H_2,aa}} H_2 + Y_{\mathrm{aa}}C_5H_7O_2N$	R_5*
Hydrogen utilization	
$4H_2 + 2CO_2 \rightarrow CH_4 + 2H_2O$	R_6
$10H_2 + 5CO_2 + NH_3 \rightarrow C_5H_7O_2N + 8H_2O$	R_7

178   *R_5 is an overall reaction resulting from weighing the fermentation reactions of individual amino acids.

179

180   Table 1 shows that VFA production from glucose utilization occurs *via* reactions R_1-R_3. The
181   pattern of the fermentation is determined by the flux allocation of glucose utilization through
182   these three reactions. We denote λ_k as the molar fraction of the sugars utilized *via* reaction
183   k. It follows that $\lambda_1 + \lambda_2 + \lambda_3 = 1$.
184   The fermentation pattern (represented in our model by the flux allocation parameters λ_k) is
185   controlled by thermodynamic conditions and by electron-mediating cofactors such as
186   nicotinamide adenine dinucleotide (NAD) that drive anaerobic metabolism via the transfer of
187   electrons in metabolic redox reactions (Mosey, 1983; Hoelzle *et al.*, 2014; van Lingen *et al.*,
188   2019). In our model, the regulation exerted by the NADH/NAD+ couple on the flux allocation
189   is incorporated *via* regulation functions that are dependent on the hydrogen partial pressure
190   ($p_{\mathrm{H_2}}$). This hybrid approach resulted by assuming a linearity between the couple NADH/NAD+
191   and the $p_{\mathrm{H_2}}$ following the work of (Mosey, 1983; Costello *et al.*, 1991). As discussed by (van
192   Lingen *et al.*, 2019), the production of acetate *via* the reaction R_1 is favoured at low
193   NADH/NAD+ while the production of propionate *via* the reaction R_2 is favoured at high
194   NADH/NAD+. Accordingly, we represented the flux allocation parameters by the following
195   sigmoid functions:

196

197
$$\lambda_1 = 1 - \frac{1}{1+\exp\left(-p_5\cdot\left(p_{\mathrm{H_2}}+p_6\right)\right)} \tag{7}$$

198

199
$$\lambda_2 = \frac{p_7}{1+\exp\left(-p_8 \cdot (p_{H_2}+p_9)\right)} \tag{8}$$

200 Our model then predicts that high levels of supplementation of *A. taxiformis* will result in high
201 hydrogen levels that will favour propionate production (R$_2$) over acetate production (R$_1$). By
202 this parameterization of the flux allocation parameters, our model accounts for the
203 concomitant reduction of the acetate:propionate ratio that is observed when methane
204 production is reduced.
205

2.3. Parameter estimation

207 We used the maximum likelihood estimator that minimizes the following objective function
208

209
$$J(\mathbf{p}) = \sum_{k=1}^{n_y} \frac{n_{t,k}}{2} \ln \left[\sum_{i=1}^{n_{t,k}} [y_k(t_{i_k}) - y_{m_k}(t_{i_k}, \mathbf{p})]^2 \right] \tag{9}$$

210

211 Where $\mathbf{p}$ is the vector of parameters to be estimated, n_y is the number of measured variables,
212 $n_{t,k}$ is the number of observation times of the variable k, t_{i_k} is the ith measurement time for
213 the variable y_k, and y_{m_k} is the value predicted by the model. The measured variables are the
214 concentrations of acetate, butyrate, propionate, NH$_3$, and the moles of methane produced.
215 We used the IDEAS Matlab® toolbox (Muñoz-Tamayo *et al.*, 2009) (freely available at
216 http://genome.jouy.inra.fr/logiciels/IDEAS) to generate the function files for solving the
217 optimization problem locally. Then, we used the generated files by IDEAS to look for global
218 optimal solutions using the Matlab optimization toolbox MEIGO (Egea *et al.*, 2014) that
219 implements the enhanced scatter search method developed by (Egea *et al.*, 2010) for global
220 optimization.
221

222 We reduced substantially the number of parameters to be estimated by setting most of the
223 model parameters to the values reported in the original model implementation and using the
224 information obtained from the *in vitro* study (Chagas *et al.*, 2019). For example, the hydrolysis
225 rate constant for NDF was obtained from (Chagas *et al.*, 2019) whereas the hydrolysis rate
226 constants of NSC ($k_{hydr,nsc}$) and proteins ($k_{hydr,pro}$) were included in the parameter
227 estimation problem. The kinetic rate constant for hydrogen utilization k_{m,H_2} was set 16
228 mol/(mol h) using an average value of the values we obtained for the predominant archaea
229 *Methanobrevibacter ruminantium* and *Methanobrevibacter smithii* (Muñoz-Tamayo *et al.*,
230 2019) using a microbial yield factor of 0.006 mol biomass/mol H$_2$ (Pavlostathis *et al.*, 1990).
231 With this strategy, we penalize the goodness-of-fit of the model. But, on the other hand, we
232 reduce practical identifiability problems typically found when calibrating biological kinetic-
233 based models (Vanrolleghem *et al.*, 1995). The parameter vector for the estimation is then $\mathbf{p}$:
234 $\{k_{hydr,nsc}, k_{hydr,pro}, k_{br}, \ p_1, p_2, \cdots p_9\}$. The optimization was set in a multi-experiment fitting
235 context that integrates the data of all treatments. To evaluate the model performance, we
236 computed the determination coefficient (R^2), the Lin's concordance correlation coefficient
237 (CCC) (Lin, 1989), the Root mean squared error (RMSE) and the coefficient of variation of the
238 RMSE (CV$_{RMSE}$). We also performed residual analysis for bias assessment according to (St-
239 Pierre, 2003).

3. Results

3.1. Dynamic prediction of rumen fermentation

242   The extended model developed in the present work to account for the impact of *A. taxiformis*
243   on the rumen fermentation is freely available at https://doi.org/10.5281/zenodo.4090332
244   with all the detailed information of the model and the experimental data used for model
245   calibration. An open source version in the Scilab software (https://www.scilab.org/) was made
246   available to facilitate reproductibility since Scilab files can be opened with a text editor. The
247   software R (https://www.r-project.org/) was used to plot the figures.
248   Figure 2 shows the dynamic data of fermentation variables for the levels of *A. taxiformis* at
249   0.06% and 0.5% compared against the model predicted variables. Figure 3 displays the
250   comparison of all observations against model predictions. Figure 4 shows the residuals for all
251   variables against centred predicted values.
252   To evaluate the performance of our model and its validation, external independent data is
253   required. Due to data limitation, we did not perform such a validation. To provide indicators
254   of our model, we calculated standard statistical indicators of model performance which are
255   shown in Table 2. These statistic indicators are biased and thus should be looked with caution
256   since they are calculated using the calibration data. Nevertheless, they provide an indication
257   of the adequacy of the model structure to represent the fermentation dynamics. For methane,
258   butyrate and NH_3 the mean and linear biases were not significant at the 5% significance level.
259   Acetate and propionate exhibited significant linear bias. The liquid compounds have an
260   average coefficient of variation of the RMSE (CV(RMSE)) of 11.25%. Methane had the higher
261   CV(RMSE) (31%). The concordance correlation coefficients were higher than 0.93. Propionate
262   had the lowest determination coefficient (R^2=0.82) while methane and the other compounds
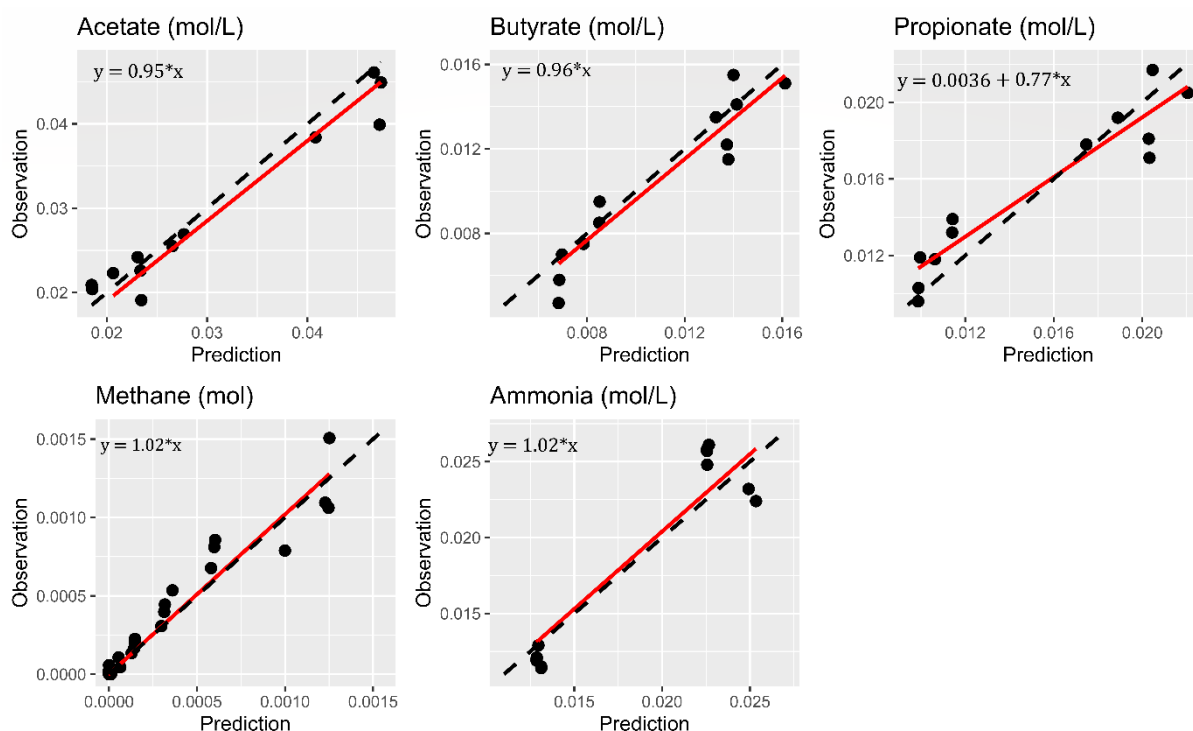263   had a R^2 close to 0.9.

264
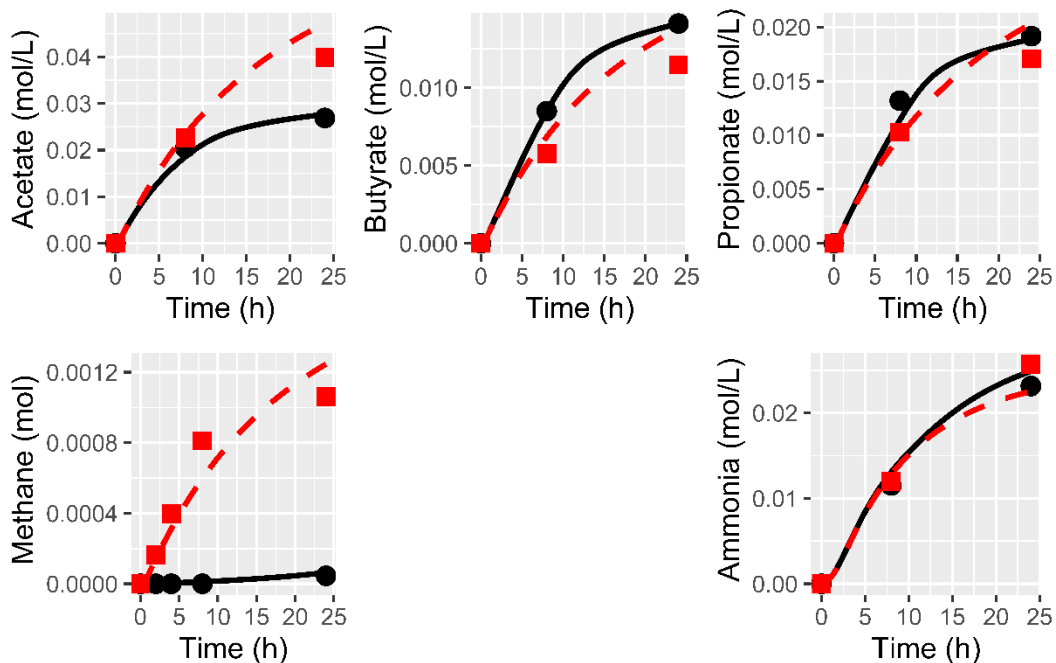
265
266

267   **Figure 2.** Example of model fitting. Experimental data of fermentation variables for the levels
268   of *A. taxiformis* at 0.5% (●) and 0.06% (■) are compared against the model predicted responses
269   in solid black lines (for 0.5% level) and in dashed red lines (for the 0.06% level).

270

Figure 3. Summary of the model performance calibration integrating data of all treatments. Experimental data (•) are plotted against the model predicted variables. Solid lines are the linear fitted curve. Dashed lines are the isoclines. Only the intercept of the curve of propionate was different from zero at 5% significance level.
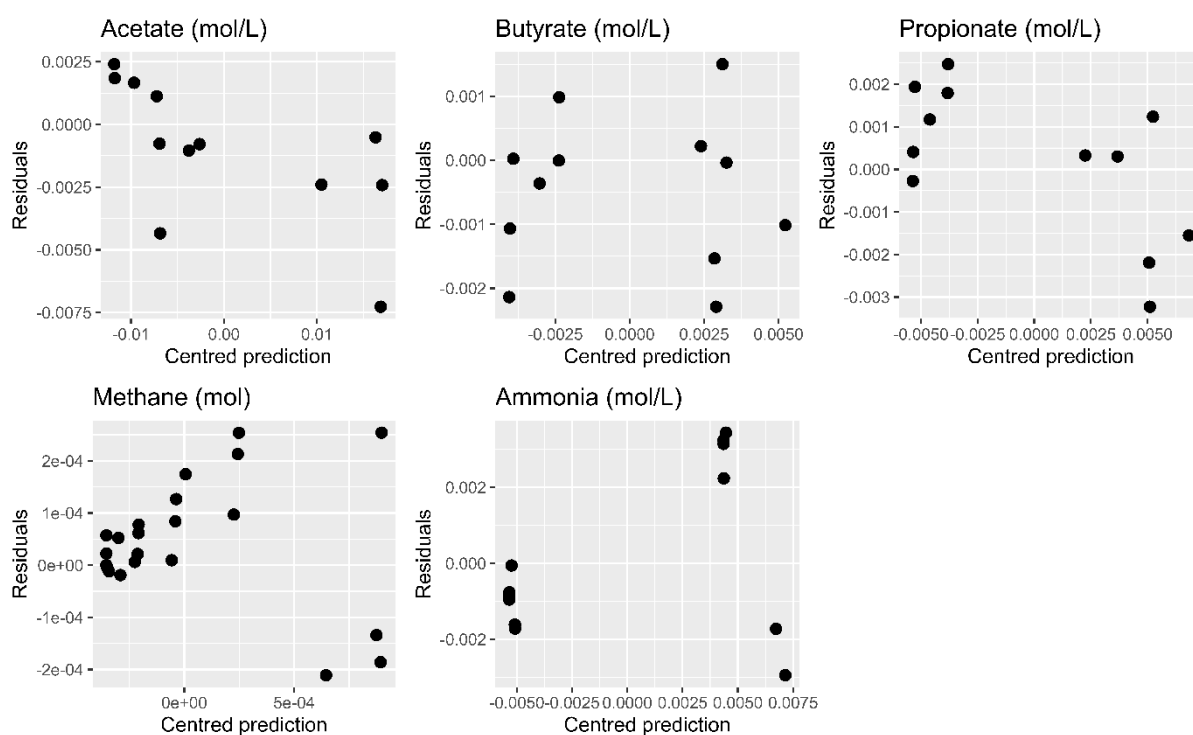
Figure 4. Residuals values of observed variables against centred predicted variables (n_{CH4} =24, $n_{NH3} = n_{ac} = n_{bu} = n_{pr}$ = 12).

283 **Table 2.** Statistical indicators of model performance.

	Acetate	Butyrate	Propionate	Methane	NH_3
R^2	0.91	0.88	0.82	0.92	0.89
RMSE[a]	0.0029	0.0012	0.0017	1.21×10^{-4}	0.002
$100 \times CV_{RMSE}$[b]	10	12	11	31	12
CCC[c]	0.96	0.94	0.93	0.96	0.93
Residual analysis					
$residual = \alpha + \beta \cdot (predicted - mean\, predicted\, value)$					
	Acetate	Butyrate	Propionate	Methane	NH_3
α (*p*-value)	-0.0010	-0.00047	0.00019	4.0e-05	0.00012
	(*p*= 0.14)	(*p*= 0.21)	(*p*= 0.63)	(*p*= 0.12)	(*p*= 0.86)
β (*p*-value)	-0.15	0.0028	-0.22	-0.031	0.15
	(*p*= 0.024)	(*p*= 0.98)	(*p*= 0.024)	(*p*= 0.60)	(*p*= 0.23)

284   [a] Root mean squared error (RMSE).

285   [b] Coefficient of variation of the RMSE (CV(RMSE)).

286   [c] Concordance correlation coefficient (CCC)

287

288 Figure 5 compares specifically the experimental data of methane against the model
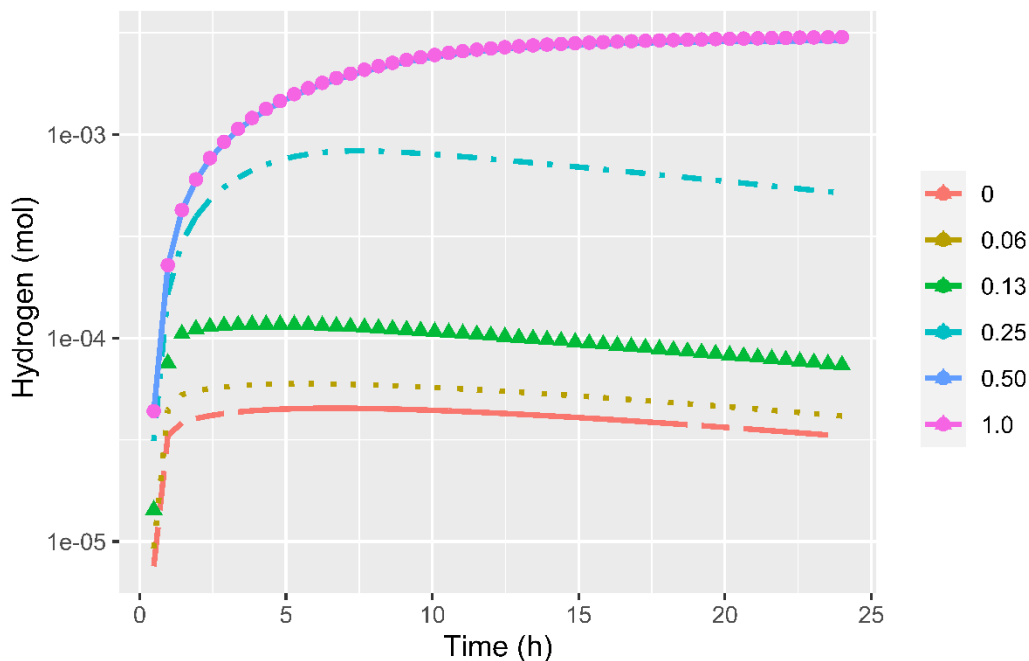289 predictions for all levels of *A. taxiformis*.

290
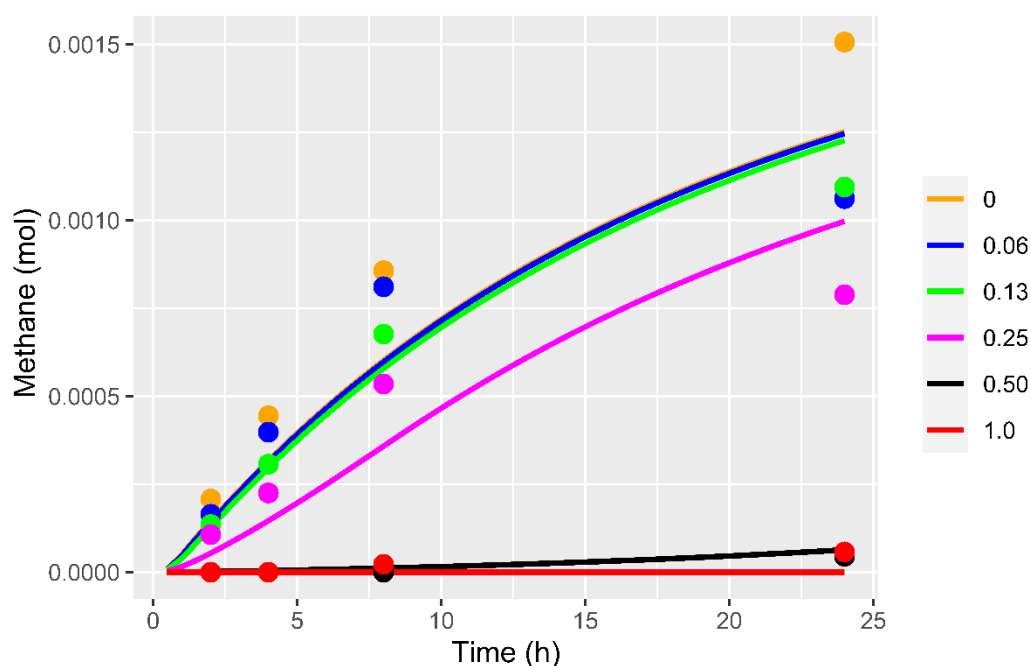
291
292 **Figure 5.** Experimental observations of methane (circles) in the headspace of the incubation
293 system are compared against the model predicted values (solid lines). Increase of the dose of
294 *A. taxiformis* results in a decrease of methane production.

295

296 3.2. Prediction of the factors representing the impact of *A. taxiformis* on rumen fermentation

298 Figure 6 plots the factors that represent the effect of *A. taxiformis* on rumen fermentation.
299 Direct inhibition of the methanogenesis due to the anti-methanogenic action of bromoform
300 is represented by the factor I_{br}. Methanogenesis inhibition results in hydrogen accumulation
301 impacting the flux allocation of sugars utilization.
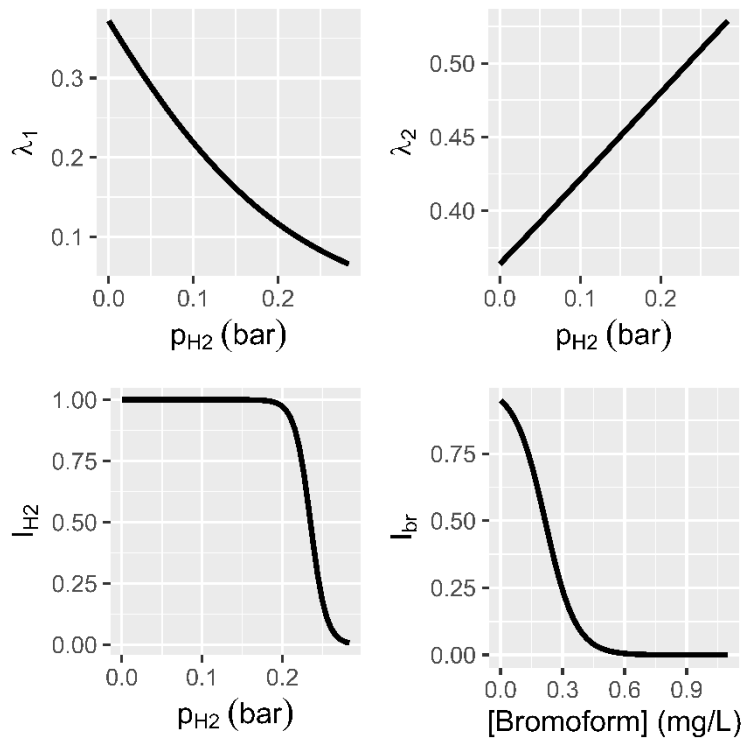
Figure 6. In our model, the effect of *A. taxiformis* on rumen fermentation is represented by a direct inhibitory effect of bromoform (I_{br}) on the methanogens growth rate. Methanogenesis inhibition results in hydrogen accumulation. Hydrogen control impacts sugar utilization by inhibiting the rate of sugar utilization (factor I_{H_2}) and by regulating the flux allocation parameters (λ_1, λ_2) towards VFA production.

Figure 7 displays the simulated dynamics of hydrogen in the headspace for all the supplementation levels of *A. taxiformis.* For supplementation levels higher than 0.25%, the methanogenesis inhibition resulted in a substantial hydrogen accumulation.

Figure 7. Predicted dynamics of hydrogen in the headspace for levels of *A. taxiformis*. Increase of the dose of *A. taxiformis* results in an increase of hydrogen in the incubation system.

4. Discussion

The goal of this work was to model the impact of *A. taxiformis* supplementation on the rumen microbial fermentation and methane production under *in vitro* conditions using experimental data from (Chagas *et al.*, 2019). Overall, our model was able to capture the dynamics of VFA, ammonia and methane production for different levels of *A. taxiformis* indicating the potential of the model structure towards the development of predictive models for assessing methane mitigation strategies in ruminants. With the exception of propionate, the slope of observed vs predicted variables is very close to one. Model limitations will be discussed further. We modelled the effect of *A. taxiformis* on rumen fermentation by two mechanisms. The first mechanism is associated to the direct inhibition of the methanogens growth rate by the anti-methanogenic compounds of *A. taxiformis* documented in different studies (Kinley *et al.*, 2016; Machado *et al.*, 2016a; Roque *et al.*, 2019). In our model, we ascribed the inhibitory effect of *A. taxiformis* only to the concentration of bromoform. The first-order kinetic rate for bromoform consumption and the inhibition factor (I_{br}) (Fig. 6) allowed our model to account for the observed dynamic decline in methanogenesis inhibition (Kinley *et al.*, 2016). It should be noted that although bromoform is the most abundant anti-methanogenic compound in *A. taxiformis*, the anti-methanogenic capacity of *A. taxiformis* is the result of the synergetic action of all halogenated products present in the macroalgae (Machado *et al.*, 2016b) . Accordingly, it will be useful to include further in our model other secondary compounds such as dibromochloromethane. To enhance our model, it will be central to perform new experiments to characterize the dynamics of anti-methanogenic compounds. This aspect is of great relevance to allow the model to be adapted to different applications of seaweed supplementation since it is known that the composition of halogenic compounds can vary with respect to the season, harvesting and drying methods.

The second mechanism that accounts for the impact of *A. taxiformis* on the fermentation is hydrogen control, which it is discussed below.

4.1.   Methane inhibition and hydrogen control

The anti-methanogenic capacity of *A. taxiformis* is dose-dependent. The experimental study of (Chagas *et al.*, 2019) showed that methane production was inhibited almost completely by *A. taxiformis* at a level of 0.5%. Our model predictions aligned with the experimental observations (Fig. 5). The anti-methanogenic capacity of the macroalgae leads to hydrogen accumulation (Kinley *et al.*, 2020; Roque *et al.*, 2020) as predicted by our model in Fig. 7. The level of hydrogen increases as the dose of *A. taxiformis* increases. The predicted values of hydrogen levels in the headspace for low doses of *A. taxiformis* showing in Figure 7 are in agreement with *in vitro* reported values (Serment et al., 2016). The level of hydrogen can impact electron-mediating cofactors such as nicotinamide adenine dinucleotide (NAD) which are important drivers of anaerobic metabolism *via* the transfer of electrons in metabolic redox reactions (Hoelzle et al., 2014). van Lingen et al., 2019 extended the rumen model developed by (Dijkstra *et al.*, 1992) to incorporate the regulation of NADH/NAD+ on the fermentation.

355 In our model, the regulation of NADH/NAD+ was incorporated *via* the control of hydrogen
356 partial pressure assuming a linearity between the couple NADH/NAD+ and the p_{H_2} and
357 following the model structure proposed by (Mosey, 1983) with a different parameterisation
358 for the functions describing the effect of p_{H_2} on the rate of glucose utilization and on the flux
359 allocation. The linearity assumption between NADH/NAD+ and the p_{H_2} might not be fulfilled
360 for all values of p_{H_2} (De Kok et al., 2013). In the experimental conditions used in the
361 experiment here analysed (Chagas et al., 2019) and under rumen physiological conditions, the
362 linearity between NADH/NAD+ might be valid.

363 With regard to the hydrogen control on glucose utilization, our model predicts that the
364 inhibition is effective at p_{H_2} higher than 0.2 bar (factor I_{H_2} in Fig. 6). In our model, the
365 incorporation of the inhibitory effect of hydrogen was motivated to account for the decrease
366 of the total production of VFA at high levels of supplementation of *A. taxiformis* observed by
367 (Chagas *et al.*, 2019). Such a decrease of VFA production is dose-dependent as observed in *in*
368 *vitro* studies (Kinley *et al.*, 2016; Machado *et al.*, 2016a). *In vivo*, while insignificant changes in
369 total VFA concentration between a control diet and diets with *A. taxiformis* supplementation
370 were observed in Brangus steers (Kinley *et al.*, 2020), inclusions of *A. taxiformis* resulted in a
371 decrease in total VFA ruminal concentration in sheep compared with control diet (Li *et al.*,
372 2016). Accordingly, additional studies with simultaneous measurements of VFA and hydrogen
373 are needed to validate the relevance of the inhibitory term I_{H_2} of our model both under *in*
374 *vitro* and *in vivo* conditions.

375 In addition to the impact of *A. taxiformis* supplementation on methane reduction, it is
376 important to look at the effects on animal productivity. *A. taxiformis* impacts the production
377 of VFAs, which are energy sources for the animal. Accordingly, changes in VFA production
378 might result in changes on productivity and feed efficiency. Optimal feeding strategies should
379 thus be designed to attain a trade-off between low methane emissions and high productivity
380 and animal health. Studies showing the effect of *A. taxiformis* supplementation on live weight
381 (Li *et al.*, 2016), average daily weight gain and feed conversion efficiency (Kinley *et al.*, 2020;
382 Roque *et al.*, 2020) are still scarce to provide a large data base for concluding on the impact
383 of *A. taxiformis* on animal productivity and feed efficiency. However, the studies of (Kinley *et*
384 *al.*, 2020; Roque *et al.*, 2020) suggest that feed conversion efficiency tend to increase
385 concomitantly with the reduction of methane production induced by an adequate
386 supplementation of *A. taxiformis*, supporting the theory of redirection of energy otherwise
387 lost as methane (Kinley *et al.*, 2020). An opportunity to enhance the action of *A. taxiformis*
388 might be the implementation of a feeding strategy integrating macroalgae supplementation
389 with an adequate additive allowing to redirect metabolic hydrogen towards nutritional
390 fermentation products beneficial to the animal. Such a strategy will fulfil the objectives of
391 reducing methane emissions while increasing animal productivity (Ungerfeld, 2020).
392
393 With regard to the fermentation pattern, when the hydrogen level increases the hydrogen
394 control operates by increasing the flux of carbon towards propionate (λ_2) while the flux
395 towards the reaction that produces only acetate (λ_1) decreases (Fig. 6). Incorporating
396 hydrogen control on the fermentation pattern in our model enabled us to predict the decrease
397 of the acetate to propionate ratio observed at levels of *A. taxiformis* supplementation leading
398 to substantial methane reduction both *in vitro* (Machado *et al.*, 2016a; Chagas *et al.*, 2019)
399 and *in vivo* (Kinley *et al.*, 2020) . Our model is also consistent with *in vitro* (Kinley *et al.*, 2016;

400   Machado *et al.*, 2016a) and *in vivo* (Stefenoni *et al.*, 2021) studies showing the increase of
401   butyrate level when the inclusion of *A. taxiformis* increases.

4.2.   Model limitations and perspectives

403   In our model, the quantification of the impact of *A. taxiformis* was ascribed by the action of
404   bromoform on the methanogens growth rate and by the action of p_{H_2} on the fermentation
405   pattern. However, in the experimental study of (Chagas *et al.*, 2019), nor bromoform nor
406   p_{H_2} were measured. From our bibliography search, we did not find studies reporting dynamic
407   measurements of bromoform. Although we did not perform an identifiably analysis, we might
408   expect that the lack of bromoform and hydrogen data in our work might result in structural
409   identifiability (Muñoz-Tamayo *et al.*, 2018) and model distinguishability problems (Walter and
410   Pronzato, 1996). We will then require external data to validate our model. Experiments to be
411   done within the MASTER project (https://www.master-h2020.eu/contact.html) will fill this
412   gap and provide data for challenging and improving our model.

413   Our model aligns with the efforts of enhancing the dynamic prediction of ruminal metabolism
414   *via* the incorporation of thermodynamics and regulation factors (Offner and Sauvant, 2006;
415   Ghimire *et al.*, 2014; van Lingen *et al.*, 2019). While our work focused only on hydrogen control
416   on sugars metabolism, future work is needed to incorporate the impact of *A. taxiformis*
417   supplementation on amino acids fermentation. The study of (Chagas *et al.*, 2019) showed a
418   decrease of branched-chain volatile fatty acids (BCVFA) with increased supplementation of *A.*
419   *taxiformis*. Such a decrease of BCVFA might have a negative influence on microbial activity.

420   We modelled the regulation of sugars metabolism by hydrogen control following a grey-box
421   modelling approach where the regulation factors were assigned to sigmoid functions without
422   an explicit mechanistic interpretation. However, to enhance the understanding of rumen
423   fermentation, it will be useful to pursue an approach incorporating the role of internal
424   electron mediating cofactors on the direction of electrons towards hydrogen or VFA (Hoelzle
425   *et al.*, 2014; Ungerfeld, 2020). Recent progress in this area (van Lingen *et al.*, 2019) opens a
426   direction for improving the prediction of rumen models.

427   The ultimate goal of this work is to pursue a model extension to account for *in vivo* conditions.
428   In this endeavour, experimental data in semi-continuous devices such as the Rusitec (Roque
429   *et al.*, 2019a) will be instrumental for model improvement. *In vivo*, in addition to the impact
430   on fermentation, *A. taxiformis* can induce changes in rumen mucosa (Li *et al.*, 2016). These
431   mucosa changes might translate in changes on the rate of absorption of ruminal VFA. This
432   effect on the rate of VFA absorption should be quantified and incorporated into an extended
433   model. In our model, the pH was set constant. However, pH exhibits a dynamic behaviour that
434   can impact the activity of the rumen microbiota. The impact of the pH on the rumen microbial
435   groups should be then considered in a future version of the model, integrating the mechanistic
436   calculation of pH elaborated in our previous model (Muñoz-Tamayo *et al.*, 2016).

437

438

439

440 Finally, although our model developments focused on the impact of *A. taxiformis* on rumen
441 fermentation and methane production, we think our model structure has the potential to be
442 applied to other additives such as 3-nitrooxypropanol (Hristov *et al.*, 2015; Duin *et al.*, 2016)
443 whose action is specifically directed to inhibit methanogenic archaea, as the halogenated
444 compounds of *A. taxiformis*. We expect these model developments can be useful to help the
445 design of sustainable nutritional strategies promoting healthy rumen function and low
446 environmental footprint.

5. Conclusions

448 We have developed a rumen fermentation model that accounts for the impact of *A. taxiformis*
449 supply on *in vitro* rumen fermentation and methane production. Our model was effective in
450 representing the dynamics of VFA, ammonia and methane for six supplementation levels of
451 *A. taxiformis*, providing a promising prediction tool for assessing the impact of additives such
452 as seaweeds on rumen microbial fermentation and methane production in *vitro*.

6. Declarations

454 **Ethics approval**: Not applicable

Availability of data and material

456 The datasets and codes used in this study are available at
457 https://doi.org/10.5281/zenodo.4090332

Funding

Acknowledgements

Authors' contributions

470 JCC, MH and SJC produced the experimental data of the study. RMT developed the
471 mathematical model and drafted the article. All authors contributed to the analysis and
472 interpretation of the results. All authors read and approved the final manuscript.

473

Conflict of interest disclosure

The authors of this article declare that they have no financial conflict of interest with the content of this article. Rafael Muñoz-Tamayo is editor of PCI Animal Science.

7. References

Beauchemin, K.A., Ungerfeld, E.M., Eckard, R.J., and Wang, M. (2020) Review: Fifty years of research on rumen methanogenesis: Lessons learned and future challenges for mitigation. *Animal* **14(S1)**: S2–S16.

Chagas, J.C., Ramin, M., and Krizsan, S.J. (2019) In vitro evaluation of different dietary methane mitigation strategies. *Animals* **9**: 1120.

Chalupa, W. (1977) Manipulating Rumen Fermentation. *J Anim Sci* **46**: 585–599.

Costello, D.J., Greenfield, P.F., and Lee, P.L. (1991) Dynamic Modeling of a Single-Stage High-Rate Anaerobic Reactor .1. Model Derivation. *Water Res* **25**: 847–858.

Czerkawski, J.W. and Breckenridge, G. (1975) New inhibitors of methane production by rumen micro-organisms. Development and testing of inhibitors in vitro. *Br J Nutr* **34**: 429–446.

Denman, S.E., Tomkins, N.W., and McSweeney, C.S. (2007) Quantitation and diversity analysis of ruminal methanogenic populations in response to the antimethanogenic compound bromochloromethane. *FEMS Microbiol Ecol* **62**: 313–322.

Dijkstra, J., Neal, H.D., Beever, D.E., and France, J. (1992) Simulation of nutrient digestion, absorption and outflow in the rumen: model description. *J Nutr* **122**: 2239–2256.

Dubois, B., Tomkins, N.W., D. Kinley, R., Bai, M., Seymour, S., A. Paul, N., and Nys, R. de (2013) Effect of Tropical Algae as Additives on Rumen *in Vitro* Gas Production and Fermentation Characteristics. *Am J Plant Sci* **4**: 34–43.

Duin, E.C., Wagner, T., Shima, S., Prakash, D., Cronin, B., Yáñez-Ruiz, D.R., et al. (2016) Mode of action uncovered for the specific reduction of methane emissions from ruminants by the small molecule 3-nitrooxypropanol. *Proc Natl Acad Sci U S A* **113**: 6172–6177.

Egea, J.A., Henriques, D., Cokelaer, T., Villaverde, A.F., MacNamara, A., Danciu, D.P., et al. (2014) MEIGO: An open-source software suite based on metaheuristics for global optimization in systems biology and bioinformatics. *BMC Bioinformatics* **15**: 136.

Egea, J.A., Martí, R., and Banga, J.R. (2010) An evolutionary method for complex-process optimization. *Comput Oper Res* **37**: 315–324.

Ellis, J.L., Dijkstra, J., France, J., Parsons, A.J., Edwards, G.R., Rasmussen, S., et al. (2012) Effect of high-sugar grasses on methane emissions simulated using a dynamic model. *J Dairy Sci* **95**: 272–285.

Evans, F.D. and Critchley, A.T. (2014) Seaweeds for animal production use. *J Appl Phycol* **26**:

509   891–899.

510   Ghimire, S., Gregorini, P., and Hanigan, M.D. (2014) Evaluation of predictions of volatile fatty
511   acid production rates by the Molly cow model. *J Dairy Sci* **97**: 354–362.

512   Hoelzle, R.D., Virdis, B., and Batstone, D.J. (2014) Regulation mechanisms in mixed and pure
513   culture microbial fermentation. *Biotechnol Bioeng* **111**: 2139–2154.

514   Hristov, A.N., Oh, J., Giallongo, F., Frederick, T.W., Harper, M.T., Weeks, H.L., et al. (2015) An
515   inhibitor persistently decreased enteric methane emission from dairy cows with no
516   negative effect on milk production. *Proc Natl Acad Sci U S A* **112**: 10663–10668.

517   Huws, S.A., Creevey, C.J., Oyama, L.B., Mizrahi, I., Denman, S.E., Popova, M., et al. (2018)
518   Addressing global ruminant agricultural challenges through understanding the rumen
519   microbiome: past, present, and future. *Front Microbiol* **9**: 2161.

520   Janssen, P.H. (2010) Influence of hydrogen on rumen methane formation and fermentation
521   balances through microbial growth kinetics and fermentation thermodynamics. *Anim
522   Feed Sci Technol* **160**: 1–22.

523   Kettle, H., Holtrop, G., Louis, P., and Flint, H.J. (2018) microPop: Modelling microbial
524   populations and communities in R. *Methods Ecol Evol* **9**: 399–409.

525   Kinley, R.D., Martinez-Fernandez, G., Matthews, M.K., de Nys, R., Magnusson, M., and
526   Tomkins, N.W. (2020) Mitigating the carbon footprint and improving productivity of
527   ruminant livestock agriculture using a red seaweed. *J Clean Prod* **259**: 120836.

528   Kinley, R.D., De Nys, R., Vucko, M.J., MacHado, L., and Tomkins, N.W. (2016) The red
529   macroalgae Asparagopsis taxiformis is a potent natural antimethanogenic that reduces
530   methane production during in vitro fermentation with rumen fluid. *Anim Prod Sci* **56**:
531   282–289.

532   Li, X., Norman, H.C., Kinley, R.D., Laurence, M., Wilmot, M., Bender, H., et al. (2016)
533   Asparagopsis taxiformis decreases enteric methane production from sheep. *Anim Prod
534   Sci* **58**: 681–688.

535   Lin, L.I. (1989) A concordance correlation-coefficient to evaluate reproducibility. *Biometrics*
536   **45**: 255–268.

537   van Lingen, H.J., Fadel, J.G., Moraes, L.E., Bannink, A., and Dijkstra, J. (2019) Bayesian
538   mechanistic modeling of thermodynamically controlled volatile fatty acid, hydrogen and
539   methane production in the bovine rumen. *J Theor Biol* **480**: 150–165.

540   Machado, L., Magnusson, M., Paul, N.A., Kinley, R., de Nys, R., and Tomkins, N. (2016a) Dose-
541   response effects of Asparagopsis taxiformis and Oedogonium sp. on in vitro
542   fermentation and methane production. *J Appl Phycol* **28**: 1443–1452.

543   Machado, L., Magnusson, M., Paul, N.A., Kinley, R., de Nys, R., and Tomkins, N. (2016b)
544   Identification of bioactives from the red seaweed Asparagopsis taxiformis that promote
545   antimethanogenic activity in vitro. *J Appl Phycol* **28**: 3117–3126.

546 Machado, L., Magnusson, M., Paul, N.A., De Nys, R., and Tomkins, N. (2014) Effects of marine
547   and freshwater macroalgae on in vitro total gas and methane production. *PLoS One* **9**:
548   e85289.

549 Machado, L., Tomkins, N., Magnusson, M., Midgley, D.J., de Nys, R., and Rosewarne, C.P.
550   (2018) In Vitro Response of Rumen Microbiota to the Antimethanogenic Red Macroalga
551   Asparagopsis taxiformis. *Microb Ecol* **75**: 811–818.

552 Maia, M.R.G., Fonseca, A.J.M., Oliveira, H.M., Mendonça, C., and Cabrita, A.R.J. (2016) The
553   potential role of seaweeds in the natural manipulation of rumen fermentation and
554   methane production. *Sci Rep* **6**: 32321.

555 Makkar, H.P.S., Tran, G., Heuzé, V., Giger-Reverdin, S., Lessire, M., Lebas, F., and Ankers, P.
556   (2016) Seaweeds for livestock diets: A review. *Anim Feed Sci Technol* **212**: 1–17.

557 Mosey, F.E. (1983) Mathematical-Modeling of the Anaerobic-Digestion Process - Regulatory
558   Mechanisms for the Formation of Short-Chain Volatile Acids from Glucose. *Water Sci*
559   *Technol* **15**: 209–232.

560 Muñoz-Tamayo, R., Giger-Reverdin, S., and Sauvant, D. (2016) Mechanistic modelling of in
561   vitro fermentation and methane production by rumen microbiota. *Anim Feed Sci*
562   *Technol* **220**: 1–21.

563 Muñoz-Tamayo, R., Laroche, B., Leclerc, M., and Walter, E. (2009) IDEAS: A parameter
564   identification toolbox with symbolic analysis of uncertainty and its application to
565   biological modelling. In, *IFAC Proceedings Volumes*., pp. 1271–1276.

566 Muñoz-Tamayo, R., Popova, M., Tillier, M., Morgavi, D.P., Morel, J.P., Fonty, G., and Morel-
567   Desrosiers, N. (2019) Hydrogenotrophic methanogens of the mammalian gut:
568   Functionally similar, thermodynamically different—A modelling approach. *PLoS One* **14**:
569   e0226243.

570 Muñoz-Tamayo, R., Puillet, L., Daniel, J.B., Sauvant, D., Martin, O., Taghipoor, M., and Blavy,
571   P. (2018) Review: To be or not to be an identifiable model. Is this a relevant question in
572   animal science modelling? *Animal* **12**: 701–712.

573 Offner, A. and Sauvant, D. (2006) Thermodynamic modeling of ruminal fermentations. **55**:
574   343–365.

575 Paul, N.A., De Nys, R., and Steinberg, P.D. (2006) Chemical defence against bacteria in the
576   red alga Asparagopsis armata: Linking structure with function. *Mar Ecol Prog Ser* **306**:
577   87–101.

578 Pavlostathis, S.G., Miller, T.L., and Wolin, M.J. (1990) Cellulose Fermentation by Continuous
579   Cultures of Ruminococcus-Albus and Methanobrevibacter-Smithii. *Appl Microbiol*
580   *Biotechnol* **33**: 109–116.

581 Puhakka, L., Jaakkola, S., Simpura, I., Kokkonen, T., and Vanhatalo, A. (2016) Effects of
582   replacing rapeseed meal with fava bean at 2 concentrate crude protein levels on feed

583   intake, nutrient digestion, and milk production in cows fed grass silage–based diets. *J*
584   *Dairy Sci* **99**: 7993–8006.

585 Ramin, M. and Huhtanen, P. (2012) Development of an in vitro method for determination of
586   methane production kinetics using a fully automated in vitro gas system-A modelling
587   approach. *Anim Feed Sci Technol* **174**: 190–200.

588 Roque, B.M., Brooke, C.G., Ladau, J., Polley, T., Marsh, L.J., Najafi, N., et al. (2019) Effect of
589   the macroalgae Asparagopsis taxiformis on methane production and rumen
590   microbiome assemblage. *Anim Microbiome* **1:3**:

591 Roque, B.M., Salwen, J.K., Kinley, R., and Kebreab, E. (2019) Inclusion of Asparagopsis armata
592   in lactating dairy cows' diet reduces enteric methane emission by over 50 percent. *J*
593   *Clean Prod* **234**: 132–138.

594 Roque, B.M., Venegas, M., Kinley, R., DeNys, R., Neoh, T.L., Duarte, T.L., et al. (2020) Red
595   seaweed (Asparagopsis taxiformis) supplementation reduces enteric methane by over
596   80 percent in beef steers. *bioRxiv*.

597 St-Pierre, N.R. (2003) Reassessment of Biases in Predicted Nitrogen Flows to the Duodenum
598   by NRC 2001. *J Dairy Sci* **86**: 344–350.

599 Stefenoni, H.A., Räisänen, S.E., Cueva, S.F., Wasson, D.E., Lage, C.F.A., Melgar, A., et al.
600   (2021) Effects of the macroalga Asparagopsis taxiformis and oregano leaves on
601   methane emission, rumen fermentation, and lactational performance of dairy cows. *J*
602   *Dairy Sci*.

603 Ungerfeld, E.M. (2020) Metabolic Hydrogen Flows in Rumen Fermentation: Principles and
604   Possibilities of Interventions. *Front Microbiol* **11**: 589.

605 Vanrolleghem, P.A., Vandaele, M., and Dochain, D. (1995) Practical identifiability of a
606   biokinetic model of activated-sludge respiration. *Water Res* **29**: 2561–2570.

607 Walter, E. and Pronzato, L. (1996) On the identifiability and distinguishability of nonlinear
608   parametric models. *Math Comput Simul* **42**: 125–134.

609 Wang, Y., Xu, Z., Bach, S.J., and McAllister, T.A. (2008) Effects of phlorotannins from
610   Ascophyllum nodosum (brown seaweed) on in vitro ruminal digestion of mixed forage
611   or barley grain. *Anim Feed Sci Technol* **145**: 375–395.

612 Wood, J.M., Kennedy, F.S., and Wolfe, R.S. (1968) The Reaction of Multihalogenated
613   Hydrocarbons with Free and Bound Reduced Vitamin B12. *Biochemistry* **7**: 1707–1713.

614